A Small Cross Flow Theory for Three-Dimensional, Compressible, Turbulent Boundary Layers on Adiabatic Walls

J. RICHARD SHANEBROOK*
Union College, Schenectady, N.Y.

AND

WILLIAM J. SUMNER†
Knolls Atomic Power Laboratory, Schenectady, N.Y.

A small cross flow integral method for predicting the growth of three-dimensional, compressible, turbulent boundary layers on adiabatic walls is presented. The method is based on the two momentum integral equations and the compressible entrainment equation corresponding to an orthogonal, curvilinear coordinate system based on the projections of the outer flow streamlines on the body surface. For small cross flow conditions the main flow momentum integral equation and the entrainment equation reduce to forms analogous to the axisymmetric system of equations employed by Sumner and Shanebrook in their study of flow over bodies of revolution. The cross flow momentum integral equation is integrated by assuming the cross flow profile can be described by a member of the (p_i, q_j) family of hodograph models. The method is applied to the three-dimensional flowfield measured by Hall and Dickens and it is found that good comparisons with data are obtained in the region where Hall and Dickens indicate that small cross flow conditions prevail. Moreover, it is found that, for the conditions of this paper, the present cross flow model is superior to Mager's model in the prediction of cross flow profiles.

Nomenclature

A = $-\left(\frac{\partial w/u_e}{\partial \zeta}\right)_{\zeta=1}$, negative of the slope of the hodograph at the boundary layer edge as shown in Fig. 2

B = $\left(\frac{\partial w/u_e}{\partial \zeta}\right)_{\zeta=0}$, slope of the hodograph at the wall as shown in Fig. 2

C_{f_1} = main flow skin-friction coefficient

F = $(1/u_e)(u_e \partial\delta/\partial s - v_e)$, the dimensionless rate of entrainment

g_1, g_2 = functions defined in the Appendix for the $(p_2, 0)$ subfamily of cross flow models

h_1, h_3 = metric coefficients for, respectively, curvilinear coordinates x_1 and x_3 (see Fig. 1)

$\bar{H}$ = $\int_0^\delta \frac{\rho}{\rho_e}\left(1-\frac{u}{u_e}\right)dy \Big/ \delta_{11}$

H_1 = δ_1/δ_{11}

H_2 = $(\delta-\delta_1)/\delta_{11}$

H_{2k} = $\int_0^\delta \frac{u}{u_e}dy \Big/ \int_0^\delta \frac{u}{u_e}\left(1-\frac{u}{u_e}\right)dy$

L = distance from station $x = 15$ to station $x = 40$ of Ref. 4

m = power law exponent

M = Mach number

p_i = number of consecutive zero derivatives at the wall beginning with the ith derivative

q_j = number of consecutive zero derivatives at the boundary-layer edge beginning with the jth derivative

r = recovery factor

s = arc length measured along the x_1 axis (outer flow streamline) as shown in Fig. 1

t = η/Δ

T = temperature

T_r = recovery temperature

T^* = Eckert's reference temperature

u, v, w = boundary-layer velocity components in the x_1, x_2, x_3 directions, respectively

x = distance from throat of nozzle (see Ref. 4)

X = distance measured from station $x = 15$ of Ref. 4

x_1, x_2, x_3 = orthogonal curvilinear coordinates based on the projections of the outer flow streamlines on the body surface (see Fig. 1)

y = arc length measured along the x_2 axis as shown in Fig. 1

z = arc length measured along the x_3 axis as shown in Fig. 1

δ = boundary-layer thickness

δ_1 = $\int_0^\delta \left(1-\frac{\rho u}{\rho_e u_e}\right)dy$

δ_{11} = $\int_0^\delta \left(1-\frac{u}{u_e}\right)\frac{\rho u}{\rho_e u_e}dy$

Δ = $\int_0^\delta \frac{\rho}{\rho_e}dy$

η = $\int_0^y \frac{\rho}{\rho_e}dy$

μ^* = viscosity evaluated at T^*

ρ = density

$(\tau_1)_w$ = wall shear stress component in the x_1 direction

$(\tau_3)_w$ = wall shear stress component in the x_3 direction

θ_{13} = $\int_0^\delta \frac{\rho u w}{\rho_e u_e^2}dy$

ζ = u/u_e

Subscripts

e = conditions at the outer edge of the boundary layer

w = conditions at the wall

Introduction

THE study of three-dimensional, turbulent boundary layers is of great practical importance since flowfields of this type are commonly found on swept wings, bodies at an angle of attack,

Presented as Paper 72-697 at the AIAA 5th Fluid and Plasma Dynamics Conference, Boston, Mass., June 26–28, 1972; submitted July 12, 1972; revision received December 18, 1972. The authors wish to thank M. G. Hall for providing unpublished outer flow inclination data. This work has been supported by the National Science Foundation through Grant GK-12697 for which the authors express their sincere appreciation.

Index category: Boundary Layers and Convective Heat Transfer—Turbulent.

* Associate Professor of Mechanical Engineering. Member AIAA.

† Engineer. Associate Member AIAA.

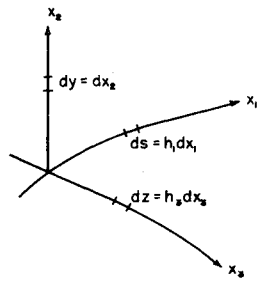

Fig. 1 Streamline coordinate system.

rotating surfaces and the bounding surfaces of internal flows. Many of the existing analyses of three-dimensional, compressible, turbulent boundary layers are based on simplifying assumptions for the cross flow velocity component within the boundary layer. For example, Bradley[1] assumed the cross flow to be small and showed that the continuity and streamwise momentum equations reduce to forms analogous to the equations describing the boundary layer on a body of revolution. This analogy has been termed the axisymmetric analogy. Bradley demonstrated that wall-cooling of the boundary layer tends to increase the momentum of the streamwise flow near the wall which in turn tends to retard the development of cross flow. This fact was previously utilized by Vaglio-Laurin,[2] who neglected the cross flow completely, in developing a theory for the three-dimensional boundary layer on a highly cooled blunt body in hypersonic flow. Another assumption made by Bradley concerning the cross flow was its form. That is, Bradley adopted Mager's[3] quadratic model

$$w/u_e = B(u/u_e)(1-y/\delta)^2 \tag{1}$$

as well as linear and cubic variations from this. However, it was noted by Bradley that Eq. (1) does not compare favorably with the adverse pressure gradient data of Hall and Dickens,[4] and concluded that a proper mathematical representation for the cross flow velocity profile was still lacking.

Other researchers who have employed Eq. (1) as cross flow model under compressible flow conditions include Braun,[5] who analyzed the flow over a slightly yawed cone, and Scott,[6] who studied the boundary-layer growth in the vortex chamber of a supersonic centrifugal compressor. Recently, as an alternative to Eq. (1), Shanebrook and Sumner[7] proposed applying the hodograph models of Refs. 8 and 9 to the cross flow velocity component of three-dimensional, compressible, turbulent boundary layers. Velocity profile comparisons were made with the experimental data of Hall and Dickens,[4] taken on a side wall of a supersonic nozzle, and the data of Rainbird,[10] taken on a yawed cone. It was found that adequate representations could be obtained for compressible cross flow profiles with (S-shaped profiles) and without (D-shaped) flow reversal.

The purpose of this paper is to develop a small cross flow integral method for three-dimensional, compressible, turbulent boundary layers on adiabatic walls based on the axisymmetric entrainment theory of Ref. 11 and the family of hodograph cross flow models described in Refs. 7–9. It will also be shown that this family of cross flow models is superior to Eq. (1) in its prediction of the cross flow under the conditions of this paper.

Small Cross Flow Approximation

In this paper the three-dimensional boundary-layer equations will be written in an orthogonal curvilinear coordinate system based on the projections of the outer flow streamlines on the body surface. Figure 1 illustrates this coordinate system where the x_1 axis is the projection of an outer flow streamline on the surface of the body and the x_3 axis lies on the body surface orthogonal to the x_1 axis. The third coordinate x_2 is measured normal to the body surface. It is customary to refer to the x_1 direction as the main flow direction and the x_3 direction as the cross flow direction.

It will be assumed throughout this paper that the cross flow velocity component w and the crosswise derivatives $\partial/\partial x_3$ are small compared with other terms in the governing partial differential equations. Based on these assumptions and order of magnitude arguments, Bradley[1] deduced in his thesis the following momentum integral equations valid for three-dimensional, compressible, turbulent boundary layers with small cross flow:

$$\frac{\partial \delta_{11}}{\delta s} + \frac{\delta_{11}}{u_e}\frac{\partial u_e}{\partial s}(H_1+2-M_e^2) + \frac{\delta_{11}}{h_3}\frac{\partial h_3}{\partial s} = \frac{(\tau_1)_w}{\rho_e u_e^2} \tag{2}$$

which is the main flow momentum integral equation and

$$\frac{\partial \theta_{13}}{\partial s} + \theta_{13}\left[\frac{(2-M_e^2)}{u_e}\frac{\partial u_e}{\partial s} + \frac{2}{h_3}\frac{\partial h_3}{\partial s}\right] + \frac{\delta_{11}}{h_1}\frac{\partial h_1}{\partial z}(H_1+1) = \frac{-(\tau_3)_w}{\rho_e u_e^2} \tag{3}$$

which is the cross flow momentum integral equation. Equation (2) is analogous to the momentum integral equation for flow over a body of revolution[11] since the equations become identical if, $h_3 = R$, where R is the radius of the body of revolution.

Consistent with the small cross flow approximation of this paper, the continuity equation corresponding to the coordinate system of Fig. 1 can be approximated by

$$\frac{\partial(\rho u)}{\partial s} + \frac{\partial(\rho v)}{\partial y} + \frac{\rho u}{h_3}\frac{\partial h_3}{\partial s} = 0$$

Integrating this equation across the boundary layer in the manner described in Ref. 12 gives

$$\frac{\partial(\delta-\delta_1)}{\partial s} = F - (\delta-\delta_1)\left[\frac{(1-M_e^2)}{u_e}\frac{\partial u_e}{\partial s} + \frac{1}{h_3}\frac{\partial h_3}{\partial s}\right] \tag{4}$$

which becomes identical with the axisymmetric entrainment equation derived by Sumner and Shanebrook[11] if h_3 is replaced by R, the radius of the body of revolution.

In the following sections a procedure for integrating the system of integral equations (2–4) will be developed, based on the compressible entrainment theory of Ref. 11 and the family of hodograph cross flow models mentioned in the Introduction. Results from the theory will then be compared with the experimental data of Ref. 4.

Solution for the Main Flow via Entrainment Theory

By integrating equations (2) and (4) along an outer flow streamline these equations can be treated as a system of two coupled, ordinary differential equations for the unknowns δ_{11} and $(\delta-\delta_1)$. That is, for such an integration, z acts as a parameter since it is maintained constant and its value merely indicates the particular streamline being followed.[13]

With Eqs. (2) and (4) effectively reduced to ordinary differential equations and the fact that they are analogous to the axisymmetric equations indicates that they can be integrated by existing methods for flow over bodies of revolution. A method of this type, based on entrainment principles, has been presented in Ref. 11 and will be adopted here.

Essentially, Ref. 11 has modified the compressible entrainment theory of Green[14] such that it relies less on empiricism and represents a simpler and more direct extension of Head's[15] incompressible entrainment theory to compressible flows. Evidence was also presented indicating the modified theory produces an improvement in accuracy. The modified theory assumes Head's incompressible entrainment relations apply to compressible flows in the following forms:

$$F = 0.0306\,(H_{2k}-3.0)^{-0.653} \tag{5}$$

and

$$H_{2k} = 1.535\,(\bar{H}-0.7)^{-2.715} + 3.3 \tag{6}$$

The applicability of these relations for three-dimensional, compressible, turbulent boundary layers has been demonstrated in Ref. 12 by comparing with the experimental data of Refs. 4 and 10. Assuming a power law velocity profile, a specific heat

ratio of 1.4 and Spence's[16] adiabatic wall temperature-velocity equation, the following relations between form parameters were presented[11].

$$H_1 = (T_r/T_e)(\bar{H}+1)-1 \tag{7}$$

$$\frac{H_2}{H_{2k}} = 1 + \frac{rM_e^2}{5}\left(\frac{H_2-1}{H_2+2}\right)\Big/\left[\frac{rM_e^2}{5}+\left(\frac{H_2+1}{2}\right)\right] \tag{8}$$

The method is completed by adopting a suitable skin-friction law such as the Ludwieg-Tillmann relation modified for compressible flow according to Eckert's reference temperature concept

$$\frac{(\tau_1)_w}{\rho_e u_e^2} = 0.123\left(\frac{\rho_e u_e \delta_{11}}{\mu^*}\right)^{-0.268}\left(\frac{T_e}{T^*}\right)10^{-0.678\bar{H}} \tag{9}$$

Equations (2 and 4–9) form a determinate system of equations and therefore can be solved to give the development of the main flow along an outer flow streamline assuming small cross flow conditions prevail.

Integration of the Cross Flow Momentum Integral Equation

With main flow quantities now determined, Eq. (3) can be integrated along an outer flow streamline provided a suitable assumption is made regarding the cross flow wall shear stress component $(\tau_3)_w$. It will be assumed that the resultant wall shear stress τ_w acts directly opposite to the resultant boundary-layer velocity vector as the wall is approached. This condition can be conveniently expressed in mathematical terms by referring to the hodograph of w/u_e vs u/u_e shown in Fig. 2. That is, defining parameter B as the slope of the hodograph at the wall it follows that

$$(\tau_3)_w = B(\tau_1)_w \tag{10}$$

This relation combined with Eq. (9) provides an empirical expression for $(\tau_3)_w$ dependent on main flow quantities δ_{11} and $\bar{H}$ as well as the cross flow parameter B. It is now necessary to find a relationship between θ_{13} and B before the integration of Eq. (3) can proceed.

From the definition of θ_{13}, it is evident that if profiles for density, main flow, and cross flow velocity components are assumed and if the cross flow profile involves the parameter B, then θ_{13} and B can be related. A family of hodograph cross flow models satisfying this requirement has been developed and compared with experimental data in Refs. 7–9 and will be adopted here for the purpose of relating these parameters.

The ability of this family to represent S-shaped cross flow profiles is primarily due to the inclusion of a second cross flow parameter A, defined in Fig. 2 as the negative of the slope of the hodograph at the outer edge of the boundary layer. Following Eichelbrenner,[17] it is assumed that parameter A obeys the differential equation

$$\frac{\partial A}{\partial s} + A^2\left(\frac{1}{u_e}\frac{\partial u_e}{\partial z}+\frac{1}{h_1}\frac{\partial h_1}{\partial z}\right)+A\left(\frac{1}{h_3}\frac{\partial h_3}{\partial s}-\frac{1}{u_e}\frac{\partial u_e}{\partial s}\right)+\frac{2}{h_1}\frac{\partial h_1}{\partial z}=0 \tag{11}$$

which can be treated as an ordinary differential equation since the only z derivatives appearing in this equation are of outer flow quantities which are considered known.

Another important feature of the hodograph family considered here is its flexibility which permits a wide variety of possible shapes for the hodograph as shown in Refs. 7 and 8. This flexibility is due to the freedom to specify the number of consecutive higher order zero derivatives at the wall and/or boundary-layer edge. That is, the conditions

$$\left(\frac{\partial^r w/u_e}{\partial \zeta^r}\right)_{\zeta=0} = 0 \qquad r = 2,3,\ldots j$$

and

$$\left(\frac{\partial^r w/u_e}{\partial \zeta^r}\right)_{\zeta=1} = 0 \qquad r = 2,3,\ldots k$$

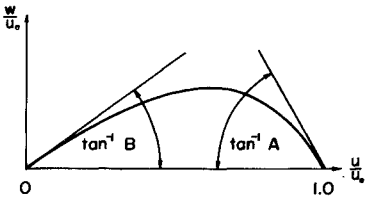

Fig. 2 Hodograph.

were used to form the family of hodograph cross flow models described in Refs. 7–9. Essentially, these conditions control the extent of experimentally observed linear regions in the hodograph plane as the wall and boundary-layer edge are approached. This family has been termed the (p_i, q_j) family of cross flow models where p_i is the number of consecutive zero derivatives at the wall beginning with the ith derivative and q_j is the number of consecutive zero derivatives at the boundary-layer edge beginning with the jth derivative. The subscripts i and j must be greater than unity and for the special case where no higher order zero derivatives are specified at the wall or boundary-layer edge a zero is substituted for p_i or q_j, respectively. Algebraic forms expressing

$$w/u_e = f(\zeta, A, B, p_2)$$

for the subfamilies $(p_2,0)$, $(p_2,q_2=1)$ and $(p_2,q_2=2)$ are given in Refs. 7 and 9.

Before the integration indicated in the definition of θ_{13} can be carried out it is necessary to assume profiles for density and the main flow boundary-layer velocity component. Assuming Spence's[16] adiabatic wall temperature relation is valid through the boundary layer and the pressure field is invariant with x_2, it follows that

$$\rho_e/\rho = T/T_e = T_r/T_e + [(T_e - T_r)/T_e](u/u_e)^2$$

which will be referred to as Spence's density relation. The main flow velocity distribution is assumed to obey the power law profile,

$$u/u_e = (\eta/\Delta)^m$$

where

$$\eta = \int_0^y \frac{\rho}{\rho_e}dy \quad \text{and} \quad \Delta = \int_0^\delta \frac{\rho}{\rho_e}dy$$

which Spence[18] found to adequately represent flat plate experimental data for a constant value of the exponent m. In this analysis m will be allowed to vary according to the relation

$$m = (\bar{H}-1)/2 \tag{12}$$

which follows from substituting this power law velocity profile into the definition of $\bar{H}$. Also, the transformed boundary-layer thickness Δ can be related to other boundary-layer thicknesses by substituting Spence's density relation into the defining equation for Δ. The result of this substitution is

$$\Delta = (T_e/T_r)\delta_1 + [(T_e - T_r)/T_r]\delta_{11} + (\delta - \delta_1) = \delta_{11}(\bar{H}+H_2) \tag{13}$$

With the power law velocity profile, Spence's density relation and a cross flow model from the (p_i, q_j) family, it is possible to perform the integration indicated in the definition of θ_{13} and thereby determine a relationship between θ_{13} and B. Such an integration has been performed in the Appendix for the $(p_2,0)$ subfamily of cross flow models with the result

$$B = (1/g_1)\theta_{13}/\Delta - (g_2/g_1)A \tag{14}$$

where g_1 and g_2 are defined in the Appendix.

With the previously determined main flow quantities and a cross flow model from the $(p_2,0)$ subfamily, Eqs. (3 and 9–14) form a determinate system which when solved give the small cross flow development along an outer flow streamline.

Application and Results

The small cross flow theory presented in this paper is mathematically described by Eqs. (2–14). Of this group, Eqs. (2–4 and

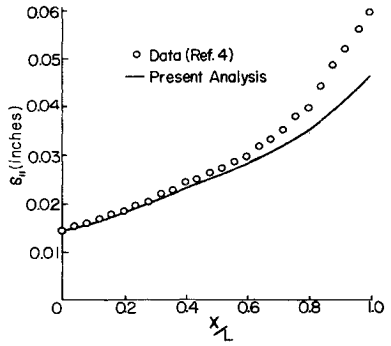

Fig. 3 Predicted values of δ_{11} compared with data of Ref. 4.

11) can be treated as ordinary differential equations and therefore solved by standard numerical integration techniques such as the Runge-Kutta method which was adopted here.

These equations have been integrated for the flow conditions of Hall and Dickens[4] who measured the three-dimensional, compressible, turbulent boundary layer on the plane, insulated, sidewall of a specially constructed supersonic nozzle. Conditions were similar to those existing on swept wings as the outer flow streamlines exhibited an inflection point which caused the formation of S-shaped cross flow profiles downstream of the inflection points. The pressure gradient imposed on the boundary layer was first favorable and then adverse.

Calculations were initiated on streamline B of Ref. 4 at station $x = 15$ by adopting starting values for δ_1, δ_{11}, θ_{13}, A, and B. With these starting values the proper cross flow model from the $(p_2, 0)$ subfamily was determined by substituting into the integrated form of the θ_{13} relation (given in the Appendix) and solving for p_2. After rounding off, this calculation indicated that the $(p_2 = 7, 0)$ cross flow model should be used at station $x = 15$ and this model was assumed to represent the cross-flow profile at all stations along streamline B.

The streamline and orthogonal curvature terms were determined from data supplied by M. G. Hall[19] giving the angle of inclination of the outer flow streamlines with respect to the x axis at each point of the 1-in. grid system described in Ref. 4. Finally, Sutherland's equation was employed throughout the calculations to account for the variation of viscosity with temperature and the recovery factor was taken to be unity.

In order to simplify the numerical integration of Eqs. (2–4 and 11), derivatives with respect to s were replaced by derivatives with respect to the Cartesian coordinate x. It is believed that this is a reasonable approximation since calculations of ds/dx

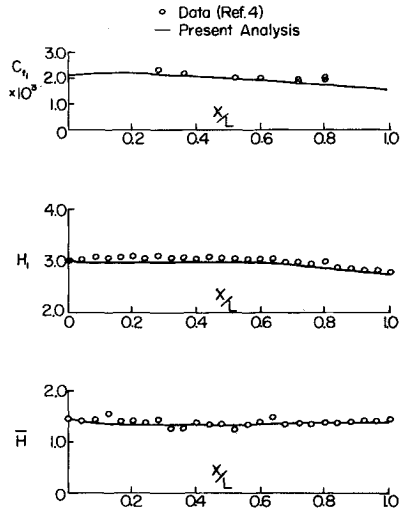

Fig. 4 Predicted values of C_{f1}, H_1 and $\bar{H}$ compared with data of Ref. 4.

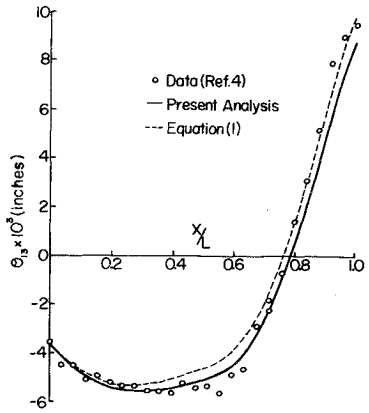

Fig. 5 Predicted values of θ_{13} compared with data of Ref. 4.

indicate that the magnitude of this derivative never exceeds 1.01 along streamline B.

These calculations were repeated using Eq. (1) for the cross flow model. This change has no effect on the main flow predictions.

Figures 3 and 4 compare the main flow parameters predicted by the present theory with the experimental values. Figures 5 and 6 compare the cross flow parameters predicted by the present theory with the experimental values and also the values found using Eq. (1). It should be noted that the abscissa of each of these figures is the ratio, X/L, where X is the distance measured from station $x = 15$ of Ref. 4 and L is the distance from station $x = 15$ to station $x = 40$ of Ref. 4. Figure 7 compares the predicted hodographs with the experimental cross flow data taken at four stations.

Conclusions

Hall and Dickens[4] compared their measurements along streamline B with the terms in the main flow momentum integral equation and concluded that small cross flow conditions prevail upstream of station $x = 30$ $(X/L = 0.6)$ on this streamline. The present results confirm this conclusion since Fig. 3 indicates that the small cross flow theory of this paper provides an adequate prediction of δ_{11} along streamline B to about station $X/L = 0.6$. Figure 4 indicates that C_{f1}, H_1, and $\bar{H}$ are predicted with good accuracy although the values for H_1 are consistently low. Therefore, it can be concluded that the axisymmetric entrainment theory of Ref. 11 provides an accurate means for predicting the main flow properties of three-dimensional turbulent boundary layers with small cross flow under the experimental flow conditions reported in Ref. 4.

The results for θ_{13}, shown in Fig. 5, indicate that both cross flow models produce relatively accurate values in the small cross flow region from $X/L = 0$ to $X/L = 0.6$. However, this is to be expected since the only term in Eq. (3) dependent on the cross

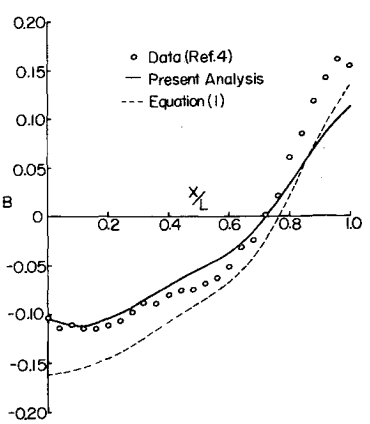

Fig. 6 Predicted values of B compared with data of Ref. 4.

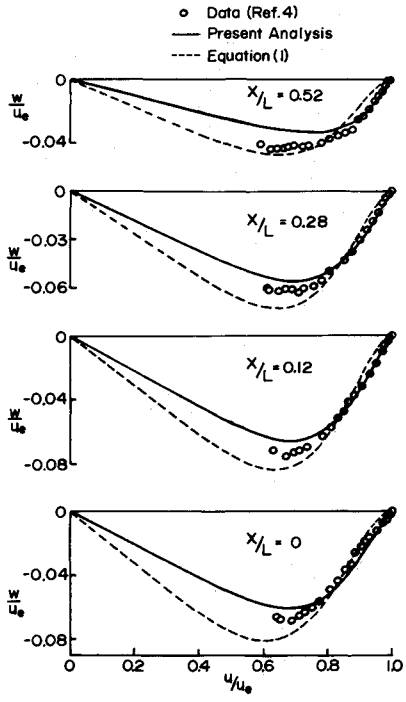

Fig. 7 Predicted hodographs compared with data of Ref. 4.

flow model is the wall shear stress term, $(\tau_3)_w$, given by Eq. (10). That is, our calculations indicate that, for the flow conditions of Ref. 4, this term is relatively small compared to the other terms in Eq. (3) and consequently has little effect on the prediction of θ_{13}. Figures 6 and 7 indicate that the present cross flow model is superior to Eq. (1) in the prediction of cross flow profiles in the small cross flow region of Ref. 4. This is expecially true in the region near the wall as evidenced by the results for cross flow parameter B shown in Fig. 6. Based on these results it can be concluded that the (p_i, q_j) family of cross flow models provides an attractive means for predicting the cross flow parameters of three-dimensional, compressible, turbulent boundary layers on adiabatic walls provided the conditions of small cross flow are satisfied.

Appendix

From the definition of η and the substitution $t = \eta/\Delta$ it follows that

$$d\eta = (\rho/\rho_e)\, dy = \Delta dt \tag{A1}$$

and the power law becomes

$$u/u_e = t^m \tag{A2}$$

Combining Eqs. (A1) and (A2) with the definition of θ_{13} gives

$$\theta_{13} = \Delta \int_0^1 t^m \frac{w}{u_e}\, dt \tag{A3}$$

where Δ is given by Eq. (13).

For the $(p_2,0)$ subfamily of models, the cross flow is given by[8,9]

$$w/u_e = B[\zeta-(p_2+2)\zeta^{p_2+2}+(p_2+1)\zeta^{p_2+3}]+A[\zeta^{p_2+2}-\zeta^{p_2+3}]$$

Combining Eq. (A2) with this cross flow model gives

$$w/u_e = B[t^m-(p_2+2)t^{m(p_2+2)}+(p_2+1)t^{m(p_2+3)}]+ A[t^{m(p_2+2)}-t^{m(p_2+3)}]$$

With this equation for w/u_e, the integrand of Eq. (A3) is simply a polynomial in t which when integrated yields

$$\theta_{13}/\Delta = g_1 B + g_2 A$$

or, solving for B

$$B = (1/g_1)\theta_{13}/\Delta-(g_2/g_1)A$$

where

$$g_1 = 1/(2m+1)-(p_2+2)/[m(p_2+3)+1]+ (p_2+1)/[m(p_2+4)+1]$$

and

$$g_2 = 1/[m(p_2+3)+1]-1/[m(p_2+4)+1]$$

References

[1] Bradley, R. G., "Approximate Solutions for Compressible Turbulent Boundary Layers in Three-Dimensional Flow," Ph.D. thesis, 1966, Georgia Inst. of Technology, Atlanta, Ga.; also *AIAA Journal*, Vol. 6, No. 5, May 1968, pp. 859–864.

[2] Vaglio-Laurin, R., "Turbulent Heat Transfer on Blunt-Nosed Bodies in Two-Dimensional and General Three-Dimensional Hypersonic Flow," *Journal of the Aerospace Sciences*, Vol. 27, No. 1, 1960, pp. 27–36.

[3] Mager, A., "Generalization of Boundary Layer Momentum Integral Equations to Three-Dimensional Flows Including Those of Rotating System," Rept. 1067, 1952, NACA.

[4] Hall, M. G. and Dickens, H. B., "Measurements in a Three-Dimensional Turbulent Boundary Layer in Supersonic Flow," RAE-TR-66214, July 1966, Royal Aircraft Establishment, England; also *Recent Developments in Boundary Layer Research*, AGARDograph 97, Pt. II, 1965, pp. 829–853.

[5] Braun, W. H., "Turbulent Boundary Layer on a Yawed Cone in a Supersonic Stream," TR R-7, 1959, NASA.

[6] Scott, B. F., "Boundary Layer Effects in the Turbulent Spiral Vortex Flow of a Compressible Fluid," *Institution of Mechanical Engineers, Proceedings*, Pt. I, Vol. 183, 1968/1969, pp. 179–186.

[7] Shanebrook, J. R. and Sumner, W. J., "Crossflow Profiles for Compressible, Turbulent Boundary Layers," *Journal of Aircraft*, Vol. 8, No. 3, March 1971, pp. 188–189.

[8] Shanebrook, J. R. and Hatch, D. E., *Transactions of the ASME, Ser. D: Journal of Basic Engineering*, Vol. 92, No. 1, March 1970, pp. 90–91.

[9] Shanebrook, J. R. and Hatch, D. E., "A Family of Hodograph Models for the Cross Flow Velocity Component of Three-Dimensional Turbulent Boundary Layers," *Transactions of the ASME, Ser. D: Journal of Basic Engineering*, Vol. 94, No. 2, June 1972, pp. 321–329.

[10] Rainbird, W. J., "Turbulent Boundary-Layer Growth and Separation on a Yawed Cone," *AIAA Journal*, Vol. 6, No. 12, Dec. 1968, pp. 2410–2416.

[11] Sumner, W. J. and Shanebrook, J. R., "Entrainment Theory for Compressible, Turbulent Boundary Layers on Adiabatic Walls," *AIAA Journal*, Vol. 9, No. 2, Feb. 1971, pp. 330–332.

[12] Shanebrook, J. R. and Sumner, W. J., "Entrainment Equation for Three-Dimensional, Compressible, Turbulent Boundary Layers," *AIAA Journal*, Vol. 10, No. 5, May 1972, pp. 693–694.

[13] Cooke, J. C. and Hall, M. G., "Boundary Layers in Three Dimensions," *Progress in Aeronautical Sciences*, Vol. 2, Pergamon Press, 1962, pp. 221–282.

[14] Green, J. E., "The Prediction of Turbulent Boundary Layer Development in Compressible Flow," *Journal of Fluid Mechanics*, Vol. 31, 1968, pp. 753–778.

[15] Head, M. R., "Entrainment in the Turbulent Boundary Layer," R and M 3152, 1958, Aeronautical Research Council, London, England.

[16] Spence, D. A., "The Growth of Compressible Turbulent Boundary Layers on Isothermal and Adiabatic Walls," R and M 3191, 1961, Aeronautical Research Council, London, England.

[17] Eichelbrenner, E. A., "La Couche Limite Tridimensionnelle en Regime Turbulent d'un Fluide Compressible: Cas de la Paroi Athermane," *Recent Developments in Boundary Layer Research*, AGARDograph 97, Pt. II, 1965, pp. 795–828.

[18] Spence, D. A., "Some Applications of Crocco's Integral for the Turbulent Boundary Layer," *Proceedings of the 1960 Heat Transfer and Fluid Mechanics Institute*, Stanford University Press, Stanford, Calif., 1960, pp. 62–76.

[19] Hall, M. G., personal communication, July 15, 1970, Royal Aircraft Establishment, Farnborough, England.